# Emergence of Quasi-Long-Range Order below the Bragg Glass Transition

N. D. Daniilidis,[1,*] S. R. Park,[1,†] I. K. Dimitrov,[1] J. W. Lynn,[2] and X. S. Ling[1,‡]

[1]*Department of Physics, Brown University, Providence, Rhode Island 02912, USA*
[2]*NIST Center for Neutron Research, Gaithersburg, Maryland 20899, USA*

(Received 27 April 2007; published 5 October 2007)

We report small angle neutron scattering rocking-curve measurements of the flux line lattices in the peak effect region in a niobium single crystal. It is found that upon cooling in a magnetic field, the transverse orientational order as well as the longitudinal translational order grow rapidly with decreasing temperature, indicating diminishing population of defects in the ordering vortex matter. Surprisingly, during subsequent warming, longitudinal order increases with increasing temperature, presumably due to annealing of flux-lattice screw dislocations. The observed behavior indicates the gradual emergence of the Bragg glass phase from entangled vortex matter in the peak effect region.

DOI: 10.1103/PhysRevLett.99.147007 PACS numbers: 74.25.Qt, 61.12.Ex

The investigation of vortex phases in type-II superconductors is interesting for understanding the behavior of these materials, as well as for studying phase transitions in disordered media. The existence of liquid [1], glasslike [2], and quasi-long-range ordered (QLRO) elastic—Bragg glass—[3,4] vortex phases has been proposed, but their properties and extent in superconducting phase diagrams are not fully understood. In this context, the peak effect, an anomalous increase in critical current as the upper critical field is approached from below, has fundamental importance: It is attributed to increased vortex pinning due to an order-disorder phase transition of the vortex lattice [5].

In neutron diffraction experiments [6], the peak effect was shown to coincide with a hysteretic order-disorder transition. Phase coexistence of ordered and disordered vortex phases has been observed in the peak effect region [7]. Moreover, the concept of phase coexistence is useful in explaining transport anomalies in the peak effect region [8]. However, direct structural information on how a Bragg glass phase with QLRO emerges from a disordered vortex phase at the Bragg glass transition is absent.

Here we report the first systematic study, using small angle neutron scattering (SANS) rocking-curve measurements, of vortex lattice correlations in the peak effect region of a niobium single crystal. Our measurements show that upon cooling in a magnetic field, the vortex state is disordered longitudinally (along the field direction) and in the transverse directions, as reported previously [6]. Over a wide temperature range below the peak effect, there is coexistence of Bragg glass with a metastable disordered phase [7]. The longitudinal correlation grows rapidly with decreasing temperature, indicating the emergence of QLRO. However, QLRO fails to be fully established on field cooling at lowest temperature. Only with subsequent warming did true QLRO (to resolution limit) appear in the vortex lattice, presumably due to annealing of the trapped defects.

The single crystal Nb sample in this work was previously studied using SANS, ac-susceptometry, calorimetry, and magnetocalorimetry [6,9]. It has nearly cylindrical shape with the [111] crystallographic direction parallel to the cylinder axis. It has zero field $T_c = 9.16$ K, extrapolated $H_{c2}(0) = 5600$ Oe, Ginzburg-Landau parameter $\kappa_1(0) = 3.4$, and residual resistivity ratio $\rho_{300}/\rho_{10} = 12$ [6,9]. These values are consistent with approximately 1 at. % concentration of oxygen impurities in the bulk [10].

The experiments were performed on the 30 m NG3 SANS instrument at the NIST Center for Neutron Research. The incident neutron wavelength was 6.0 Å with 14% (FWHM) wavelength spread. Double pinhole collimation was used and the measured neutron-beam angular spread was 0.13° FWHM. The magnet cryostat was mounted on a Huber stage, allowing for precise rotation on the horizontal plane. The angle, $\omega$, between the neutron beam and the applied magnetic field was varied in steps of 0.10° around the configuration where the neutron beam is parallel to the field, $\boldsymbol{H}$. Measurements were performed on in-field cooling (FC) down to 3.2 K and on subsequent field-cooled warming (FCW), at a fixed field of 4000 Oe.

A typical succession of SANS patterns is shown in Fig. 1, and a schematic of the scattering geometry in the inset of Fig. 2(a). In Fig. 1, six first order Bragg peaks are present, indicating the existence of an orientationally ordered flux line lattice. Each one of the observed peaks follows a curve of increasing and decreasing intensity as $\omega$ is changed. This is quantified by summation of the intensity incident in the region of the peak, for example, inside the white frame encircling the (−1,1) peak in Fig. 1(g).

In Fig. 2(a) we show the $q_x q_y$-integrated intensity versus rotation angle, of the (−1,1) Bragg peak, for different temperatures and thermal histories. We find that a good phenomenological fit to the data is a Lorentzian function $I(\omega) \propto 1/[(\omega - \omega_0)^2 + \Delta\omega^2]$. Sharper curves, for example, a Gaussian, fail to describe the tail parts of the rocking-curve data. The $I(\omega)$ curves arising from the peaks (1,0) and (−1,0), i.e., those closest to the $q_y$ axis, are not

 © 2007 The American Physical Society

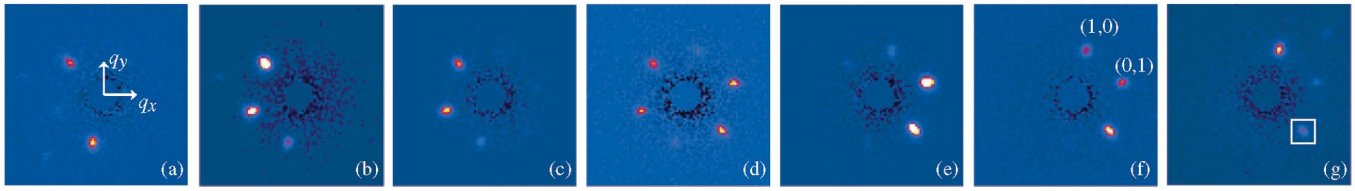


FIG. 1 (color). Typical succession of SANS patterns in a vortex lattice rocking-curve measurement. The SANS detector lies on the $xy$ plane. The data shown were obtained on FCW at $T = 3.35$ K, $H = 4000$ Oe. Rotation angles, left to right, are $\omega = -0.30°$, $-0.20°$, $-0.10°$, $0.00°$, $0.10°$, $0.20°$, $0.30°$. We use the peak labeling scheme shown in (f).

suitable for quantitative analysis, as they only include points on one side of the full curve and will result in underdetermined curve-fitting situations.

The Lorentzian-fit results serve to summarize the qualitative behavior of flux-lattice longitudinal correlations on FC and subsequent FCW. In Fig. 2(b) we show the half width $\Delta\omega$ of the Lorentzian fits performed to the data. On FC the rocking curves are wider than on FCW. Upon cooling from $T_{c2}$, $\Delta\omega$ decreases continuously, and the extrapolated value joins the FCW branch at $T_0 \approx 3.87$ K. On FCW, the half width is slightly below 0.10°. Interestingly, on warming from 3.23 K, $\Delta\omega$ follows a downward trend with increasing temperature. Moreover, the slope of $\Delta\omega(T)$ on the FCW branch changes slightly in the neighborhood of $T_0$, as seen from the linear fits shown in Fig. 2(b). The observed behavior reveals a gradual increase of longitudinal translational order on FC, and subsequent further increase on FCW. The sharpest rocking curves in the neighborhood of 4.4 K are in the resolution limit.

The hysteresis and temperature dependence in $\Delta\omega$ cannot be attributed to a demagnetization effect such as that observed in a pristine niobium crystal without the peak effect anomaly [11]. In that case, the sample shape, enhanced surface pinning, and low value of $\kappa$ would increase the demagnetization-related bending of the flux lines. Despite this, in that sample the rocking-curve widths were one half of those reported here on the FCW branch. More important, the width temperature dependence, $d(\Delta\omega)/dT$, in the earlier work [11] was 5 times smaller than that found here on FCW.

Instead, what we see in Fig. 2(b) is the process of vortex matter crystallization in the presence of disorder. The hysteresis is consistent with previous reports on the transverse structure function $S(q_x, q_y)$ of this Nb single crystal [6]. For example, in the inset of Fig. 2(b) we show the typical behavior of a Bragg peak azimuthal width, $\Delta\theta$, on the $q_x q_y$ detector. Our findings indicate that with decreasing temperature, the increasing flux line interactions lead to gradual enhancement of both longitudinal translational [Fig. 2(b)] and orientational [Fig. 2(b) inset] flux-lattice order. The hysteresis reveals a significantly higher amount of flux-lattice defects on FC than on FCW.

In order to extract quantitative information from the rocking curves, the instrumental resolution function, $R(\omega)$, is needed [12]. This can be estimated by taking into account the beam collimation and wavelength spread. In a separate study [13], the resolution function of our instrument was found to be of the empirical form $R(\omega) \propto 1/(1 + \exp[(|\omega| - \omega_c)/\Delta])$. In what follows, we empirically estimate $R(\omega)$ for every pair of inversion symmetric Bragg peaks, to be of the above form and have the half width of the sharpest rocking curve for that pair of peaks. However, even the approximation of the resolution function by a Gaussian produces essentially the same results.

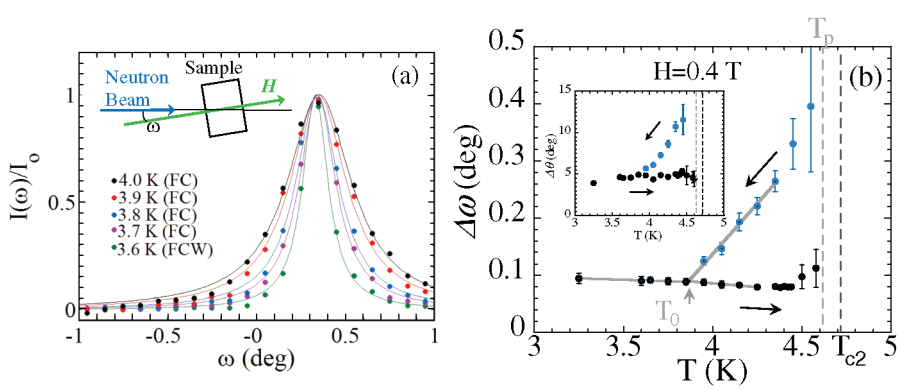


FIG. 2 (color). (a) Normalized intensity versus rotation angle for the (1, −1) Bragg peak at different temperatures on both FC and FCW paths. Also shown are fitted Lorentzian curves. Inset: Geometry of the rocking-curve measurement. (b) Half width of Lorentzian fits to the rocking-curve data. The locations of the peak of the peak effect ($T_P$) and superconducting transition ($T_{c2}$) are marked. Gray lines are linear fits performed on the data points within the ranges where the lines are drawn. Inset: Azimuthal widths of Bragg peaks on the $q_x q_y$ plane, in agreement with Ref. [6].

The convolution of the resolution function with a nonsingular structure function can sufficiently describe the central part of the measured rocking curves, but not the smooth tails at larger angles. This is evident from the dashed line fit in Fig. 2(b), where the measured curve is fitted with a Lorentzian, $L(\omega)$, convoluted with $R(\omega)$: $I(\omega) = (L * R)(\omega)$. A two-component curve of the form $I(\omega) = I_0[fR(\omega) + (1-f)(L * R)(\omega)]$, shown as a solid line in Fig. 2(b), provides a better fit, with typically two to 3 times smaller sum of squared residues. This curve accommodates both the resolution dominated central portion and the Lorentzian-like smooth tails of the curve. The slight asymmetry present in the rocking-curve (the left side of the curve is lower than the right side) is due to asymmetry in the neutron-beam angular profile, and does not undermine our central observation that a two-component curve provides a better fit to the data.

In the two-component curve, the central, resolution limited, portion [$\propto fR(\omega)$] can be accounted for by the presence of the Bragg glass phase, characterized by translational quasi-long-range order [14]. The interpretation of the Lorentzian rocking-curve tails is less straightforward. They could arise from the behavior of the flux lattice in the so-called Larkin regime [15], which is relevant for the Bragg glass phase on small length scales [4]. Alternatively, the Lorentzian tails of the curves can arise from the presence of a frozen-in entangled phase [1].

A Lorentzian component in the structure function implies exponential decay of the flux line lattice correlation function $C_{Q_0}(z) = \langle e^{iQ_0(u(z)-u(0))}\rangle \propto e^{-z/L_z}$, with longitudinal correlation length $L_z$. The width of the Lorentzian component $L(\omega) \propto 1/[(\omega-\omega_0)^2 + \Delta^2]$, allows us to determine the correlation length: For a Bragg peak located at $(Q_{0,x}, Q_{0,y})$ this is $L_z = (Q_{0,x})^{-1}\Delta$. In Fig. 3(b) we show the $L_z$ value obtained as the average of the values determined from the first order Bragg peaks, excluding (1,0) and (−1,0) for the reason mentioned earlier. Error bars are variances about the average. We find correlation lengths in the 2–9 $\mu$m range. On FC, $L_z$ shows a roughly linear increase from zero, with decreasing temperature. The temperature variation on FCW is weaker, and the value varies between 3 and 7 $\mu$m.

These $L_z$ values imply the existence of significant amounts of frozen-in flux-lattice defects which disrupt translational quasi-long range order in the flux line lattice. We estimate the longitudinal correlation length expected in the collective pinning model for the short length scale, Larkin, regime. Following the notation of Blatter *et al.* [16], the flux line displacement field follows: $\langle[u(z) - u(0)]^2\rangle = z\gamma_U/[2\pi^2\lambda\alpha_0 c_{66}\sqrt{(c_{44}c_{66})}] \equiv z\ell$, where dispersionless elastic constants can be used, and $\gamma_U \propto \langle\delta T_c^2\rangle/T_c^2$ characterizes the strength of "$\delta T_c$" pinning. If the statistical weight of the displacement field is Gaussian, the correlation function in the vicinity of reciprocal lattice point $\boldsymbol{Q}_0$ follows $C_{Q_0}(z) \propto e^{-(1/4)Q_0^2\ell z}$, and as a result the structure function is a Lorentzian: $S(q_z) \propto 1/[q_z^2 + (\frac{1}{4}Q_0^2\ell)^2]$, which yields $L_z = \alpha_0^2/(\pi^2\ell)$. For our sample we have previously determined all relevant superconducting properties, as well as the transition width $\delta T_c$ [9]. We thus estimate $L_z \approx 200$ $\mu$m.

The estimated value is significantly larger than the measured one. Even in the case of non-$\delta T_c$ pinning, such as atomic lattice defects and strain fields acting in addition to the impurity related pinning of our calculation, these mechanisms are unlikely to account for the discrepancy by a factor of 20 between the two results. Therefore, we consider unlikely the crossover to the Larkin regime as the source of the two-component rocking curves.

Instead, we attribute the reduced extent of longitudinal flux line correlations to the presence of a supercooled disordered vortex phase. In this scenario, the observed behavior is the result of *phase coexistence* in the flux lattice obtained on field cooling. The Bragg glass phase starts to crystallize with decreasing temperature, but it occupies only a fraction of the flux-lattice volume. The disordered phase consists of pinned flux lattices with frozen-in flux-lattice defects, such as edge and screw dislocations and disclinations. These defects disrupt the translational and orientational order on larger scales.

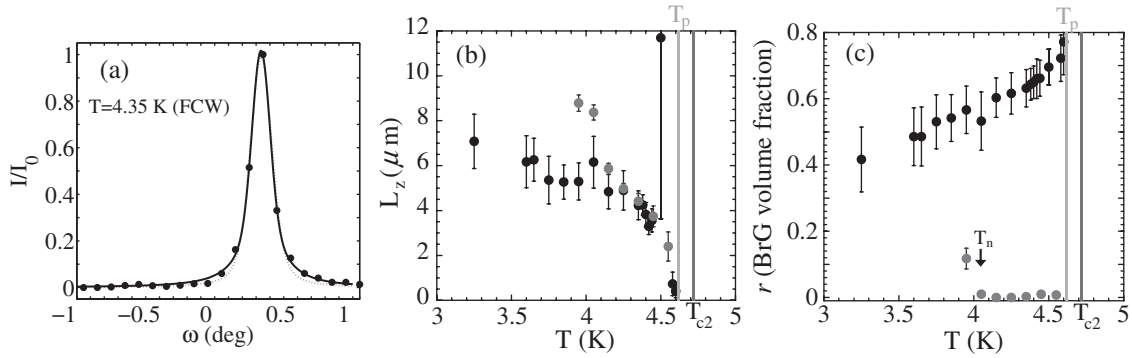


FIG. 3. (a) Fits to a FCW rocking curve. Dashed line is a Lorentzian structure function convoluted with the resolution function. Solid line is the two-component fit. (b) Longitudinal correlation length $L_z$, in the amorphous phase. Open symbols: FC, solid symbols: FCW. (c) Volume fraction of Bragg glass phase in the coexistence picture, for FCW and FC paths. The values shown in (b) and (c) are averages of values obtained from four peaks, error bars are variances about the average.

The extent of each phase present in the system is proportional to the integrated intensity of the corresponding component of the measured rocking curve. Thus we determine the fraction of Bragg glass phase as: $r \equiv \int fR(\omega)d\omega / \int [fR(\omega) + (1-f)(L * R)(\omega)]d\omega$. The results are plotted in Fig. 3(c). On FC the fraction of Bragg glass phase remains essentially zero down to approximately $T_n = 4.0$ K. Subsequently, the Bragg glass phase starts to nucleate, and its volume fraction increases to $r \approx 0.4$ at 3.23 K. Thus, the flux lattice obtained after FC down to 3.23 K has been *only partly equilibrated* to the Bragg glass phase. Upon FCW from 3.23 K, the Bragg glass fraction increases linearly with temperature, giving rise to the observed sharpening of the rocking curves shown in Fig. 2(b).

We now examine the process by which the disordered phase anneals on FC. In the inset of Fig. 2(b), we show that the Bragg peak azimuthal width decreases continuously with decreasing temperature. This process has to be interaction driven. It occurs as increasing flux line interactions cause flux-lattice edge dislocations to anneal. In the same range, the longitudinal correlation length increases from 2 to 8 $\mu$m, likely due to elasticity driven annealing of screw dislocations. On FC to 4.0 K, the azimuthal width is slightly higher than the instrumental resolution limit, and corresponds to a bond-angle spread of 1° over 40000 vortex spacings. The range of longitudinal correlations is much more limited, $L_z \approx 8$ $\mu$m, corresponding to approximately 100 vortex spacings. These structural properties of the supercooled disordered phase in the neighborhood of 4.0 K reaffirm early observations of a hexatic glass [17,18]. On cooling below $T_n = 4.0$ K, the Bragg glass nucleates from the hexatic glass phase cf. Fig. 3(c).

Although Bragg glass starts to crystallize on cooling, an amount of frozen-in entangled phase remains in the system, and the Bragg glass phase can only get further established upon subsequent warming. The interaction-driven ordering has limited effectiveness in annealing flux-lattice defects. As the temperature decreases below $T_{c2}$ the vortex line crossing energy increases [19], which means that screw dislocations become harder to anneal. As a result the metastable, entangled hexatic phase can be supercooled far below $T_n$, where Bragg glass starts to crystallize. Thus, the field-cooled flux lattice at 3.23 K contains only a fraction $r \approx 0.4$ of Bragg glass phase. Nevertheless, once the thermodynamically stable Bragg glass phase has started to nucleate, it is more effective in annealing screw dislocations than the hexatic glass. As a result, on FCW from 3.23 K the decrease in vortex cutting energy assists in further annealing of screw dislocations and the Bragg glass fraction increases considerably.

In summary, we performed structural measurements in a vortex lattice thermally cycled through the Bragg glass transition. Our results indicate coexistence of Bragg glass with the metastable disordered phase, over a large region below the peak of the peak effect. Both orientational and translational order are argued to proceed via interaction-driven annealing of flux-lattice defects. We find that orientational order is established considerably faster than translational order, giving rise to a metastable hexatic glass. The Bragg glass phase nucleates out of the latter, but fails to be fully established on field cooling. Nevertheless, on warming from a partially equilibrated Bragg glass phase, quasi-long-range order emerges.

We wish to thank Professor C. Elbaum for his interest in this work. This work was supported by NSF under Grant No. NSF-DMR-0406626 and used facilities supported by No. NSF-DMR-0454672.

*Present address: Institut für Quantenoptik und Quanteninformation, Innsbruck, Austria.
†Present address: QB3 Institute, University of California, Berkeley, CA, USA.
‡Corresponding author.
xsling@brown.edu

[1] D. R. Nelson, Phys. Rev. Lett. **60**, 1973 (1988); D. R. Nelson and H. S. Seung, Phys. Rev. B **39**, 9153 (1989); D. R. Nelson and P. Le Doussal, Phys. Rev. B **42**, 10 113 (1990); M. C. Marchetti and D. R. Nelson, Phys. Rev. B **41**, 1910 (1990).
[2] D. S. Fisher, M. P. A. Fisher, and D. A. Huse, Phys. Rev. B **43**, 130 (1991).
[3] T. Nattermann, Phys. Rev. Lett. **64**, 2454 (1990).
[4] T. Giamarchi and P. Le Doussal, Phys. Rev. Lett. **72**, 1530 (1994); T. Giamarchi and P. Le Doussal, Phys. Rev. B **52**, 1242 (1995).
[5] T. Giamarchi and S. Bhattacharya, in *High Magnetic fields: Applications to Condensed Matter Physics and Spectroscopy*, edited by C. Bertier, L. P. Levy, and G. Martinez (Springer-Verlag, Berlin, 2002) p. 314, and the references therein.
[6] X. S. Ling *et al.*, Phys. Rev. Lett. **86**, 712 (2001); S. R. Park *et al.*, Phys. Rev. Lett. **91**, 167003 (2003).
[7] M. Marchevsky, M. J. Higgins, and S. Bhattacharya, Nature (London) **409**, 591 (2001).
[8] Z. L. Xiao *et al.*, Phys. Rev. Lett. **92**, 227004 (2004).
[9] N. D. Daniilidis *et al.*, Phys. Rev. B **75**, 174519 (2007).
[10] W. DeSorbo, Phys. Rev. **132**, 107 (1963); W. DeSorbo, Phys. Rev. **134**, A1119 (1964).
[11] E. M. Forgan *et al.*, Phys. Rev. Lett. **88**, 167003 (2002).
[12] The vortex lattice longitudinal structure function $S_z(q_z) \equiv S(\boldsymbol{q}_{\perp 0}, q_z)$ enters the observed rocking curve via function $F(\omega) = S_z(q_z = \omega q_{x0})$, convoluted with the instrumental resolution function.
[13] N. D. Daniilidis, I. K. Dimitrov, and X. S. Ling, J. Appl. Crystallogr. **40**, 959 (2007).
[14] T. Klein *et al.*, Nature (London) **413**, 404 (2001).
[15] A. I. Larkin, Zh. Eksp. Teor. Fiz. **58**, 1466 (1970) [Sov. Phys. JETP **31**, 784 (1970)].
[16] G. Blatter *et al.*, Rev. Mod. Phys. **66**, 1125 (1994).
[17] C. A. Murray *et al.*, Phys. Rev. Lett. **64**, 2312 (1990).
[18] P. Kim, Z. Yao, and C. M. Lieber, Phys. Rev. Lett. **77**, 5118 (1996).
[19] C. Carraro and D. S. Fisher, Phys. Rev. B **51**, 534 (1995).